Supporting Information

Accelerated ligand-mapping molecular dynamics simulations for the detection of recalcitrant cryptic pockets and occluded binding sites

Justin Tze-Yang Ng, Yaw Sing Tan*

Bioinformatics Institute, Agency for Science, Technology and Research (A*STAR), 30 Biopolis Street, #07-01 Matrix, Singapore 138671, Singapore

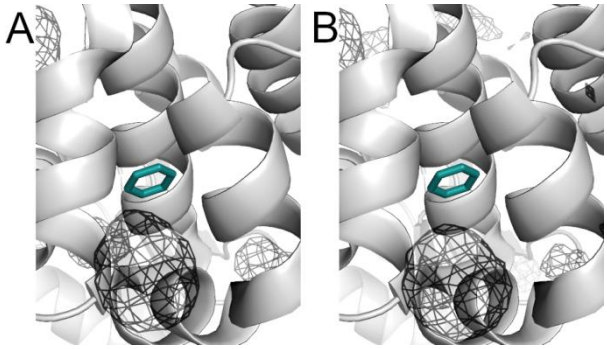

Figure S1. Benzene occupancy maps of T4 lysozyme L99A mutant generated from 10 × 50 ns of (A) aLMMD and (B) standard LMMD simulations superimposed on the ligand-bound PDB structure 4W52. Benzene occupancy maps are shown as black meshes.

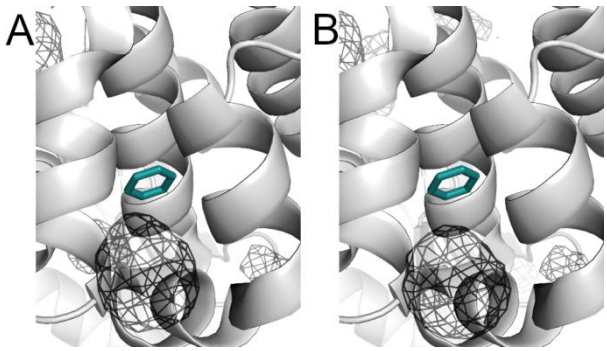

Figure S2. Benzene occupancy maps of T4 lysozyme L99A mutant generated from 20 × 50 ns of (A) aLMMD and (B) standard LMMD simulations superimposed on the ligand-bound PDB structure 4W52. Benzene occupancy maps are shown as black meshes.

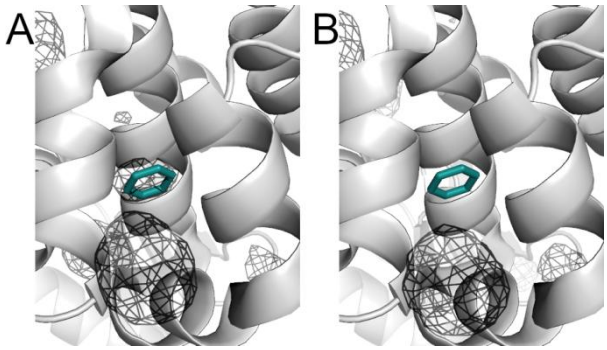

Figure S3. Benzene occupancy maps of T4 lysozyme L99A mutant generated from 20 × 200 ns of (A) aLMMD and (B) standard LMMD simulations superimposed on the ligand-bound PDB structure 4W52. Benzene occupancy maps are shown as black meshes.

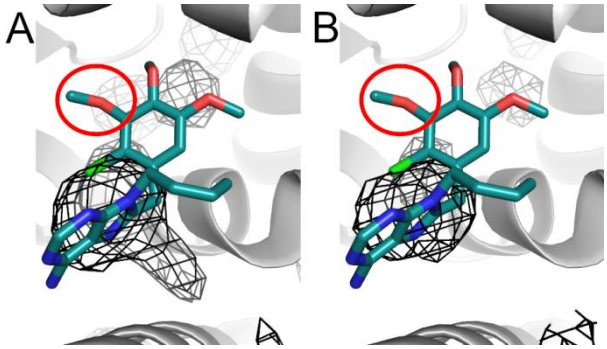

Figure S4. Benzene occupancy maps of HSP90 generated from the entire simulation length of (A) aLMMD and (B) standard LMMD simulations superimposed on the ligand-bound PDB structure 1UYD. Benzene occupancy maps are shown as black meshes. The red circles indicate the position of the cryptic pocket.

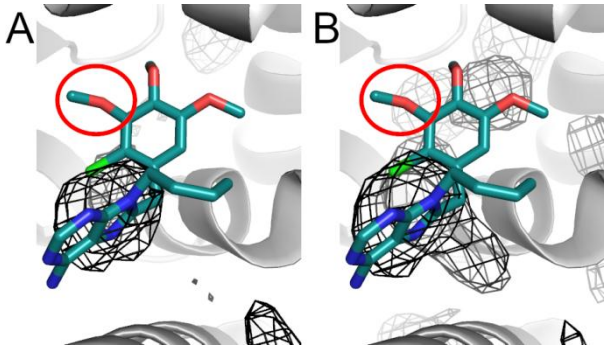

Figure S5. Benzene occupancy maps of HSP90 generated from the (A) 0–60-ns and (B) 60–130-ns analysis windows of aLMMD simulations, superimposed on the ligand-bound PDB structure 1UYD. Benzene occupancy maps are shown as black meshes. The red circles indicate the position of the cryptic pocket.

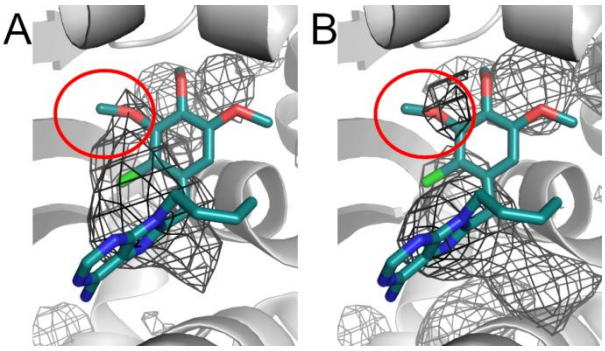

Figure S6. Benzene occupancy maps of HSP90 generated from the 130–200-ns segments of aLMMD (A) runs 1–10 and (B) runs 11–20, superimposed on the ligand-bound PDB structure 1UYD. Benzene occupancy maps are shown as black meshes. The red circles indicate the position of the cryptic pocket.

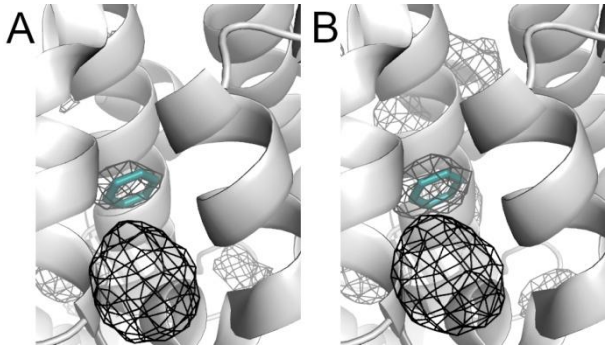

Figure S7. Benzene occupancy maps of T4 lysozyme L99A mutant generated from the 130–200-ns segments of aLMMD (A) runs 1–10 and (B) runs 11–20, superimposed on the ligand-bound PDB structure 4W52. Benzene occupancy maps are shown as black meshes.

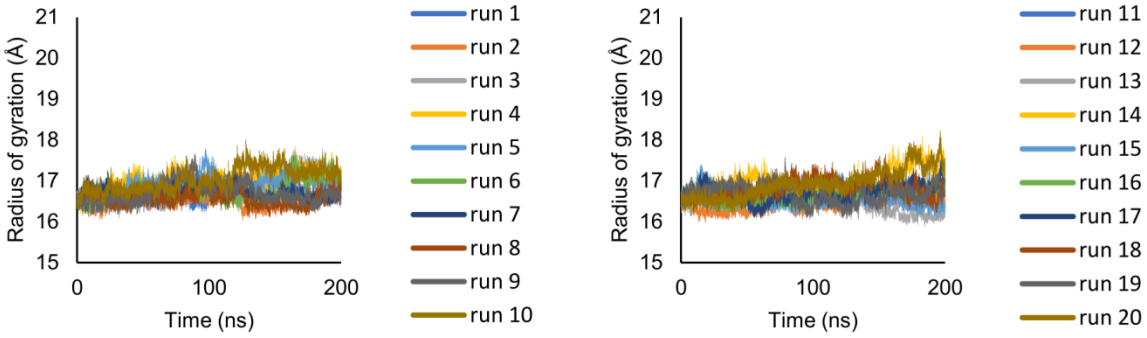

Figure S8. Radius of gyration of Cα atoms for 20 HSP90 aLMMD runs.

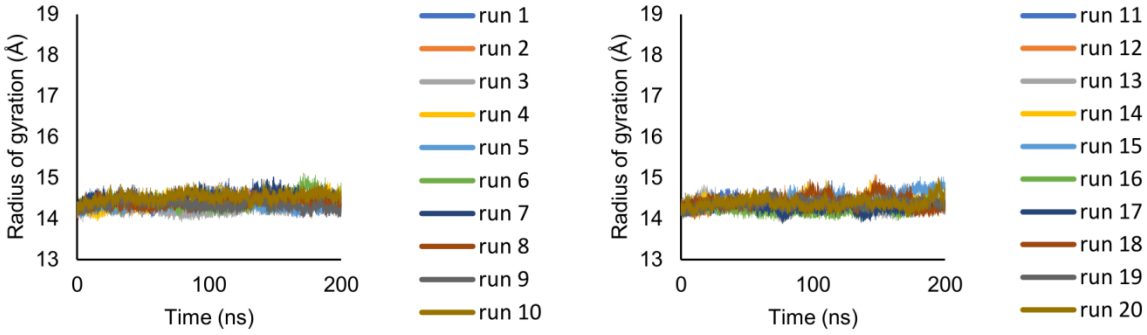

Figure S9. Radius of gyration of Cα atoms for 20 Bcl-xL aLMMD runs. Residues 28-81 were excluded from the Rg calculation as this region is highly flexible and not resolved in the initial crystal structure.

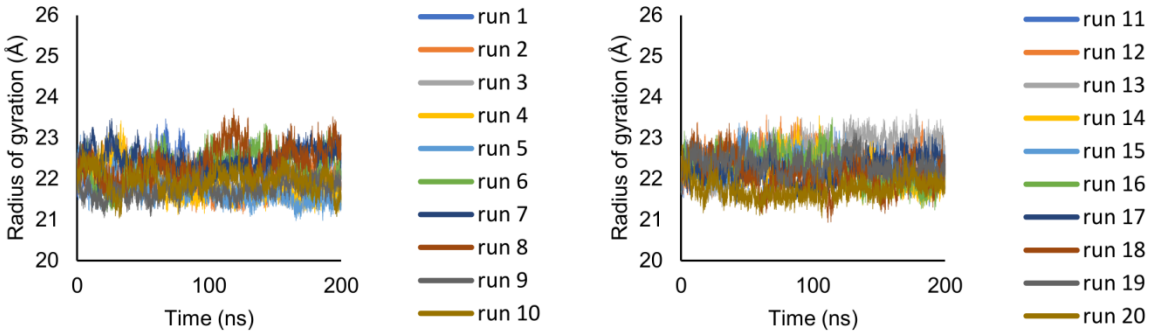

Figure S10. Radius of gyration of Cα atoms for p38 MAPK aLMMD runs.

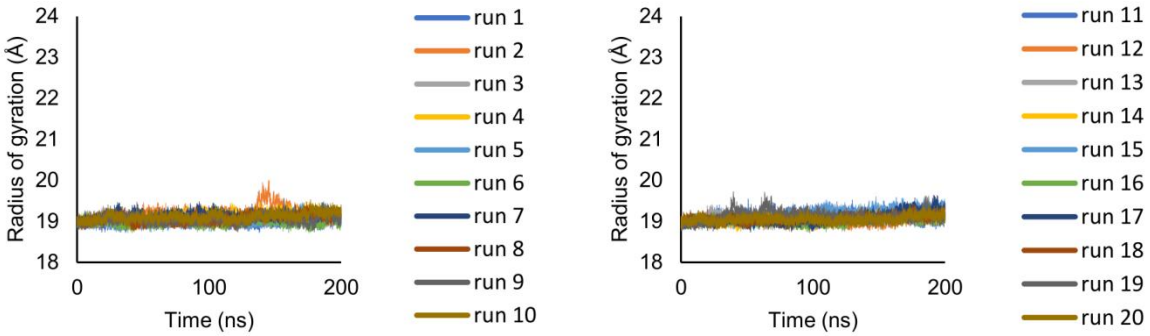

Figure S11. Radius of gyration of Cα atoms for PTP1B aLMMD runs.

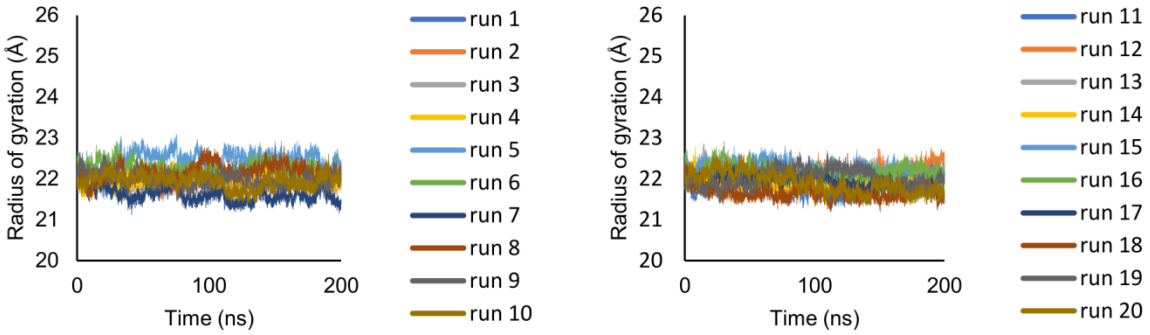

Figure S12. Radius of gyration of Cα atoms for PDK1 aLMMD runs.

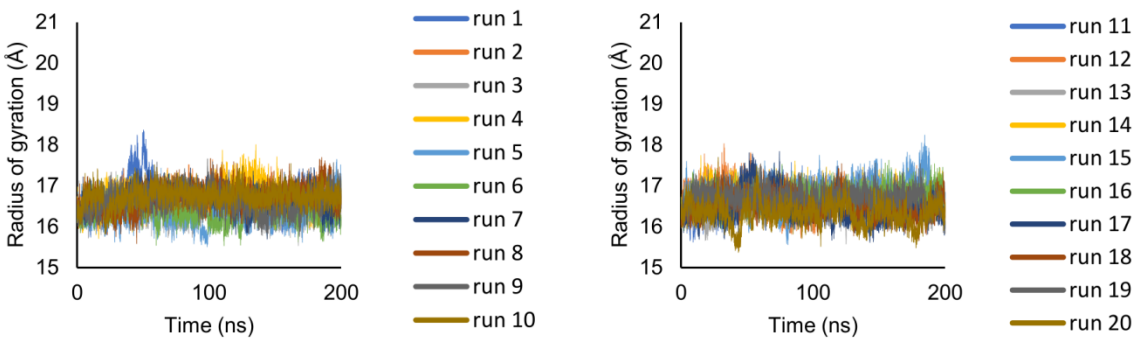

Figure S13. Radius of gyration of Cα atoms for T4 lysozyme L99A mutant aLMMD runs.

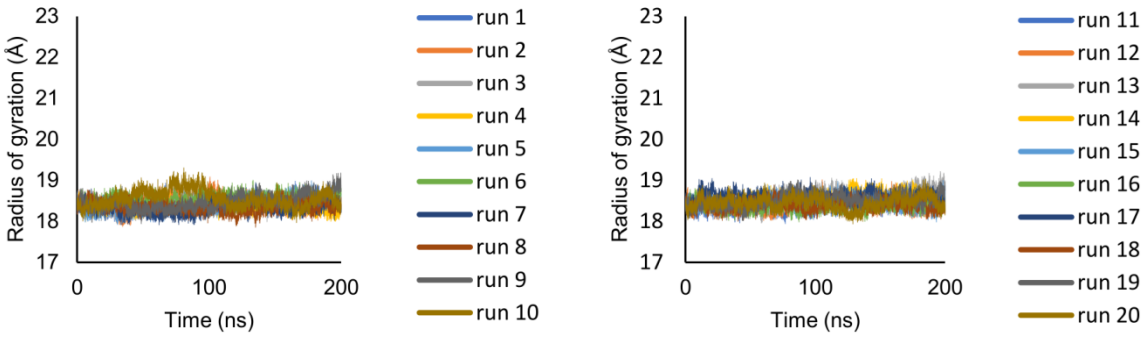

Figure S14. Radius of gyration of Cα atoms for ERα aLMMD runs.

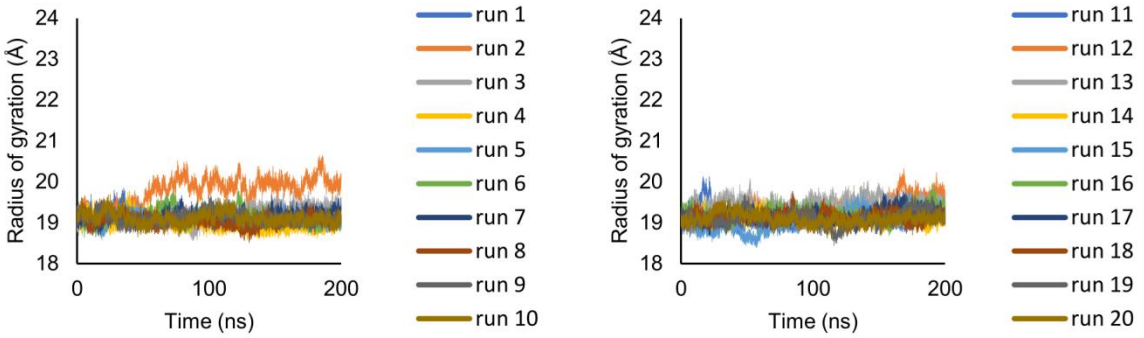

Figure S15. Radius of gyration of Cα atoms for PPAR-γ aLMMD runs.

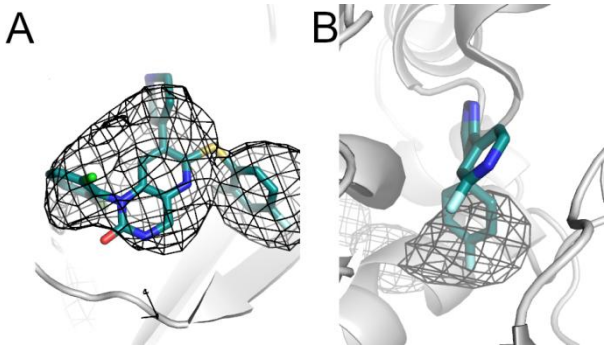

Figure S16. Ability of aLMMD to detect binding sites in p38 MAPK mapped by previous studies. (A) p38 MAPK benzene occupancy maps superimposed on the ligand-bound PDB structure 1OUY at the ATP binding site. (B) p38 MAPK benzene occupancy maps superimposed on the ligand-bound PDB structure 3HL7 at a cryptic allosteric site formed by backbone movements of loop residues 195-198. Benzene maps are shown as black meshes.

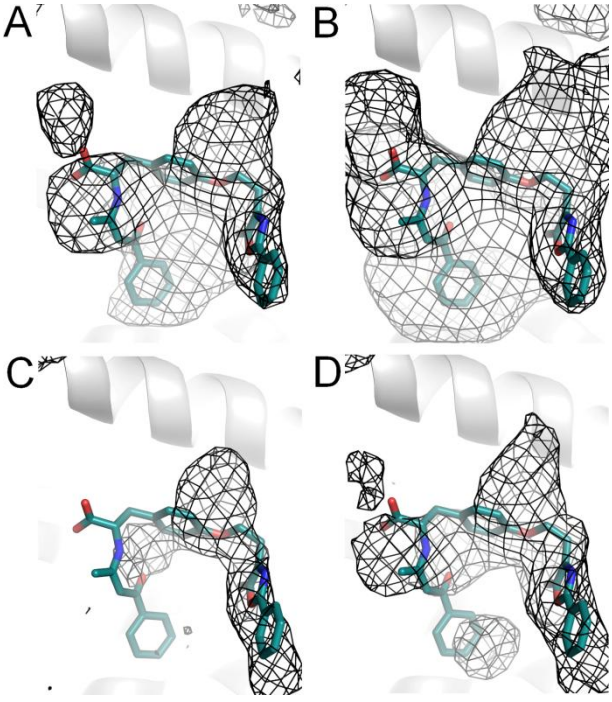

Figure S17. Benzene occupancy maps of PPAR-γ generated from the (A) 0–60-ns and (B) 60–130-ns analysis windows of aLMMD simulations, and (C) 0–60-ns and (D) 60–130-ns analysis windows of standard LMMD simulations, superimposed on the ligand-bound PDB structure 1K74. Benzene occupancy maps are shown as black meshes.

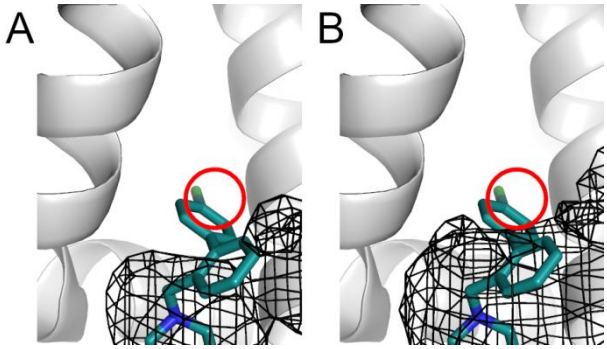

Figure S18. Benzene occupancy maps of Bcl-xL generated from the (A) 0–60-ns and (B) 60–130-ns analysis windows of aLMMD simulations, superimposed on the ligand-bound PDB structure 2YXJ. Benzene occupancy maps are shown as black meshes. The red circles indicate the position of the cryptic pocket.

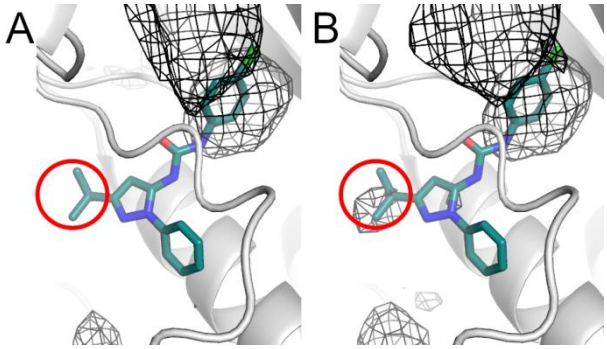

Figure S19. Benzene occupancy maps of p38 MAPK generated from the (A) 0–60-ns and (B) 60–130-ns analysis windows of aLMMD simulations, superimposed on the ligand-bound PDB structure 1W82. Benzene occupancy maps are shown as black meshes. The red circles indicate the position of the cryptic pocket.

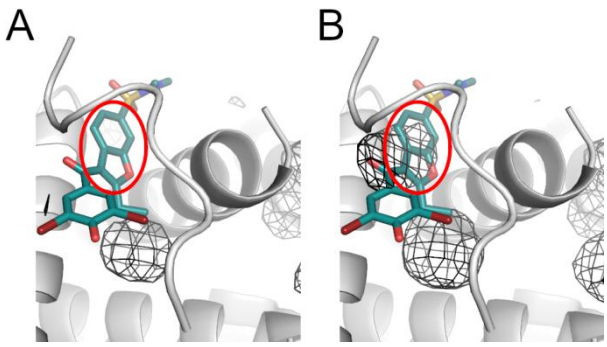

Figure S20. Benzene occupancy maps of PTP1B generated from the (A) 0–60-ns and (B) 60–130-ns analysis windows of aLMMD simulations, superimposed on the ligand-bound PDB structure 1T48. Benzene occupancy maps are shown as black meshes. The red circles indicate the position of the cryptic pocket.

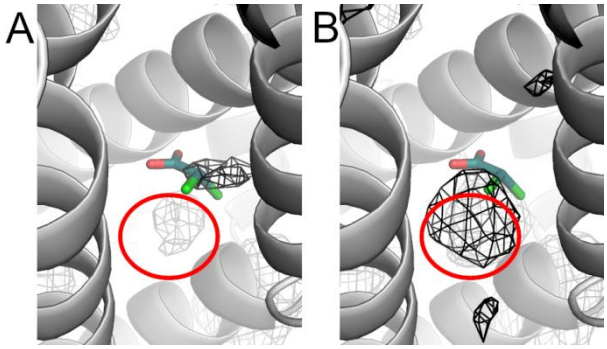

Figure S21. Benzene occupancy maps of PDK1 generated from the (A) 0–60-ns and (B) 60–130-ns analysis windows of aLMMD simulations, superimposed on the ligand-bound PDB structure 2Q8H. Benzene occupancy maps are shown as black meshes. The red circles indicate the position of the cryptic pocket.

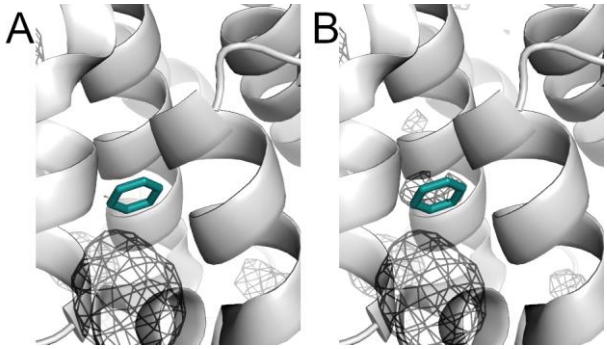

Figure S22. Benzene occupancy maps of T4 lysozyme L99A mutant generated from the (A) 0–60-ns and (B) 60–130-ns analysis windows of aLMMD simulations, superimposed on the ligand-bound PDB structure 4W52. Benzene occupancy maps are shown as black meshes.

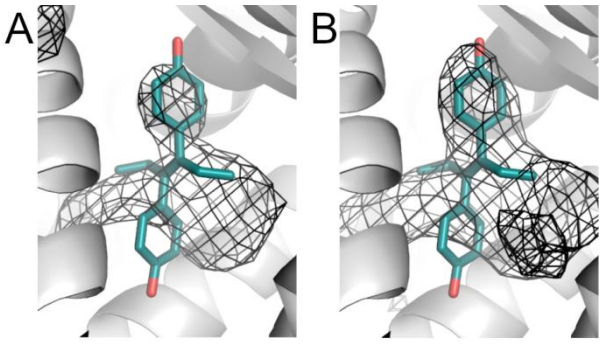

Figure S23. Benzene occupancy maps of ERα generated from the (A) 0–60-ns and (B) 60–130-ns analysis windows of aLMMD simulations, superimposed on the ligand-bound PDB structure 3ERD. Benzene occupancy maps are shown as black meshes.

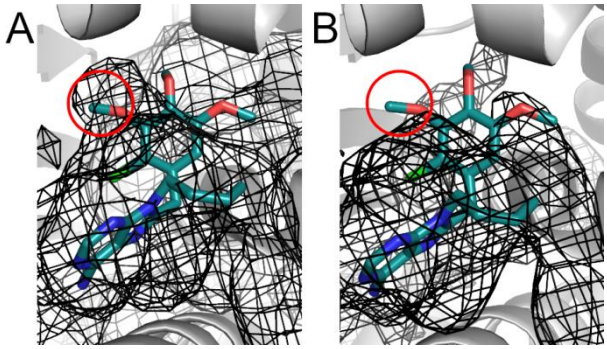

Figure S24. MDpocket density maps (isovalue 1) generated from (A) aLMMD and (B) standard aMD simulations of HSP90. The red circles indicate the position of the cryptic pocket.

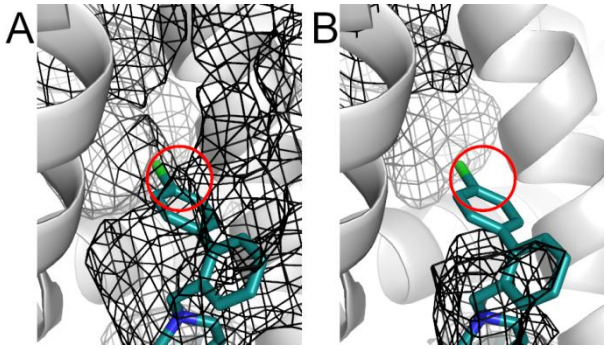

Figure S25. MDpocket density maps (isovalue 1) generated from (A) aLMMD and (B) standard aMD simulations of Bcl-xL. The red circles indicate the position of the cryptic pocket. The disordered loop region comprising residues 26-82 was excluded from the structural alignment prior to MDpocket analysis.

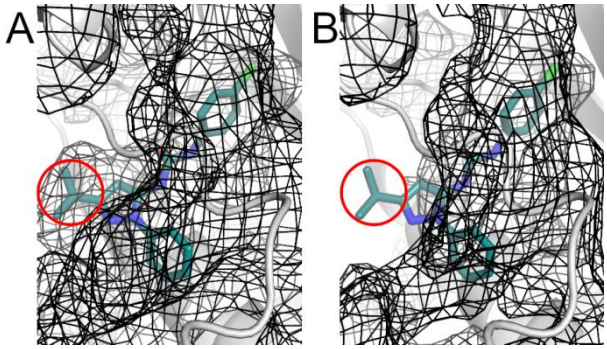

Figure S26. MDpocket density maps (isovalue 1) generated from (A) aLMMD and (B) standard aMD simulations of p38 MAPK. The red circles indicate the position of the cryptic pocket.

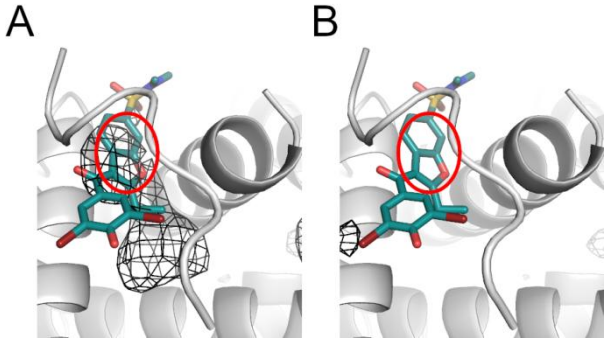

Figure S27. MDpocket density maps (isovalue 3) generated from (A) aLMMD and (B) standard aMD simulations of PTP1B. The red circles indicate the position of the cryptic pocket.

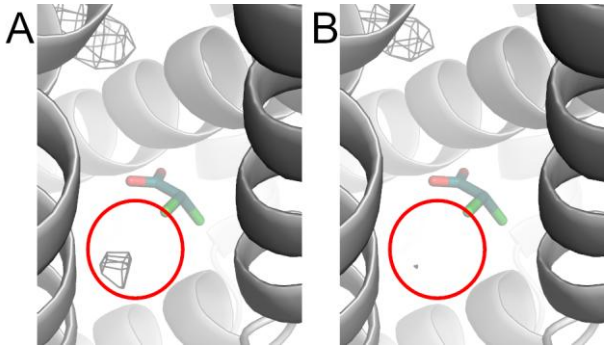

Figure S28. MDpocket density maps (isovalue 6) generated from (A) aLMMD and (B) standard aMD simulations of PDK1. The red circles indicate the position of the cryptic pocket.

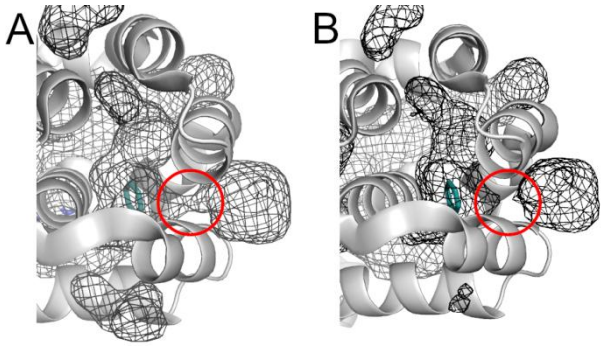

Figure S29. MDpocket density maps (isovalue 0.4) generated from (A) aLMMD and (B) standard aMD simulations of T4 lysozyme L99A mutant. The transient channel connecting the binding site to the protein surface is indicated by a red circle.

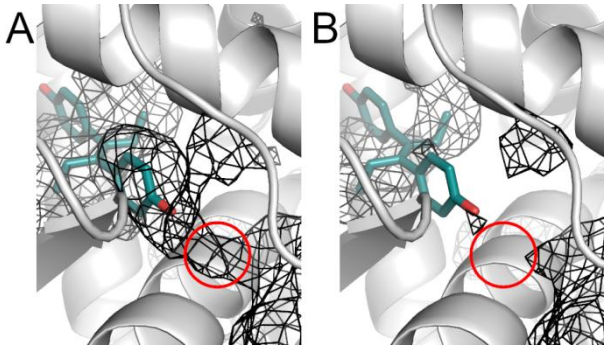

Figure S30. MDpocket density maps (isovalue 2) generated from (A) aLMMD and (B) standard aMD simulations of ERα. The transient channel connecting the binding site to the protein surface is indicated by a red circle.

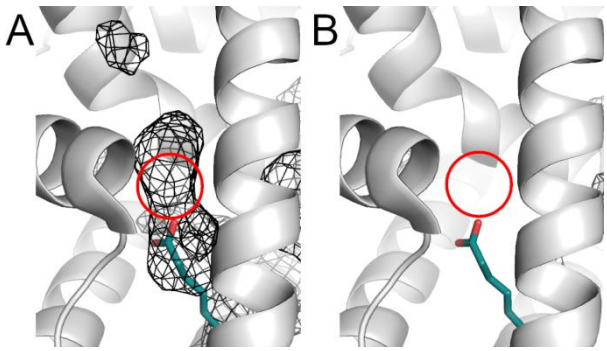

Figure S31. MDpocket density maps (isovalue 3) generated from (A) aLMMD and (B) standard aMD simulations of PPAR-γ. The transient channel connecting the binding site to the protein surface is indicated by a red circle.